

Examination of F/A-18 honeycomb composite rudders for disbond due to water using through-transmission ultrasonics

A. K. Edwards¹, S. Savage², P. L. Hungler¹ and T. W. Krause³

¹*Department of Chemistry and Chemical Engineering,
Royal Military College of Canada, Kingston, ON, Canada;
email: Alayne.Edwards@forces.gc.ca, email: Paul.Hungler@rmc.ca*

²*Quality Engineering Test Establishment, 45 Sacre-Coeur Blvd. Gatineau, Canada;
email: Steve.Savage.SJL@forces.gc.ca*

³*Department of Physics, Royal Military College of Canada, Kingston, ON, Canada;
Fax 001 613 541 6040; Phone: +1 613 541 6000 x 6415; Fax: + 613541 6040;
email: Thomas.Krause@rmc.ca*

crossref <http://dx.doi.org/10.5755/j01.u.66.2.529>

Abstract

The flight control surfaces of F/A-18 aircraft are composed of carbon/epoxy skin and aluminum honeycomb core composite material that has a known susceptibility to water ingress. The rudder has failed in flight due to moisture induced bond degradation between skin and core. Manual through-transmission Ultrasonic Testing (UT), applied to the rudder surface, currently identifies disbond as a reduction in received signal amplitude. However, water within the honeycomb cells provides significant sound transmission, which may mask disbond. In this study, water was first identified within two in-service rudders using thermography. Precise water locations were then mapped by neutron radiography. Time-base analysis of through-transmission A-scans, obtained using squirter technology, permitted discrimination of cell wall signals from signals that had passed through water within the cells. Examination of received cell wall signal intensities, modeled for disbond in the presence of water, demonstrated potential for identification of disbond even when water was present.

Keywords: aluminum honeycomb core composite, through-transmission ultrasonics, neutron radiography, thermography.

1. Introduction

The F/A-18, manufactured by McDonnell Douglas, uses a composite honeycomb sandwich panel for many of its flight control surfaces. The two rudders on the F/A-18 are located just behind each of two vertical stabilizers. Water ingress is a potential failure mechanism, as moisture introduced within the rudder's structure can degrade epoxy adhesives that bond the carbon epoxy skins to the aluminum honeycomb core, resulting in disbond of the honeycomb core [1,2]. Once the disbanded area reaches a critical size, in-flight failure can result where the majority of the rudder is torn from its hinges [3]. Fortunately, due to the F/A-18's twin tail design, this type of failure has not resulted in loss of life or air assets. It is a maintenance issue, however, due to a finite supply of rudders and their replacement cost of approximately \$75,000 from the manufacturer [4].

The rudder consists of a relatively thick lightweight aluminum honeycomb core bonded with structural grade FM300 to two stiff/thin carbon epoxy (AS4/3501-6) skins. The bonds attaching aluminum to the carbon/epoxy face sheet are designated fillet bonds. The leading edge, where the rudder attaches to the aircraft, has a titanium channel that contains holes to attach the grounding studs. The channel is bonded to the core with a foam adhesive FM404-NA. The adhesive is porous with respect to transport of water [5], permitting water to move by capillary forces and disperse parallel to the leading edge [6]. Water enters the structure through points along the leading edge, most likely at the grounding strap attach lugs

and hinge points [7]. The presence of water, and subsequent interaction with adhesives, results in eventual disbonding of the honeycomb structure from the wing skin.

Two types of water ingress in honeycomb composites have been suggested [2]. The first is liquid water in cells the result of ingress through poor seals around fasteners or directly through damaged areas of the face sheets. The second is moisture, from service environment humidity, that has diffused into the structure through the composite skin's epoxy matrix. Flat wise tension tests on coupons demonstrate that liquid water in cells degrades bonds quickly and severely [2]. However, diffused moisture, existing as moistened adhesive, does not cause the same degree of disbond and degradation takes longer to occur [2].

The primary technique used by aircraft maintenance technicians to inspect honeycomb composite material is ultrasonic through-transmission inspection. This may be performed manually, with the rudder attached to the aircraft or by application of automated scanning systems. A suitable couplant, such as water or gel, is used between transducer and test material to optimize coupling of acoustic energy into the structure. The rudder is characterized by slightly nonparallel surfaces with edges that vary in thickness from as thin as 3 mm at the trailing edge to 29 mm at the top and 61 mm at the bottom of the leading edge, where it is attached to the aircraft structure. This variation in thickness complicates interpretation of signals via time-base analysis. Fig. 1 shows a schematic cross section of the rudder consisting of dry cells and those partially filled with water in an inspection configuration.

Discontinuities in the material will attenuate or reflect the acoustic energy. The resulting A-Scan is displayed on an oscilloscope as a function of signal amplitude and time [8]. The United States Navy (USN) rudder inspection procedure, which is also applied in Canada, relies on the identification of disbonds by an observed reduction of the received signal amplitude [7]. This technique may be compromised, however, by the presence of water within the honeycomb cells, as the additional coupling provided by the water will allow a substantial signal amplitude to be transmitted.

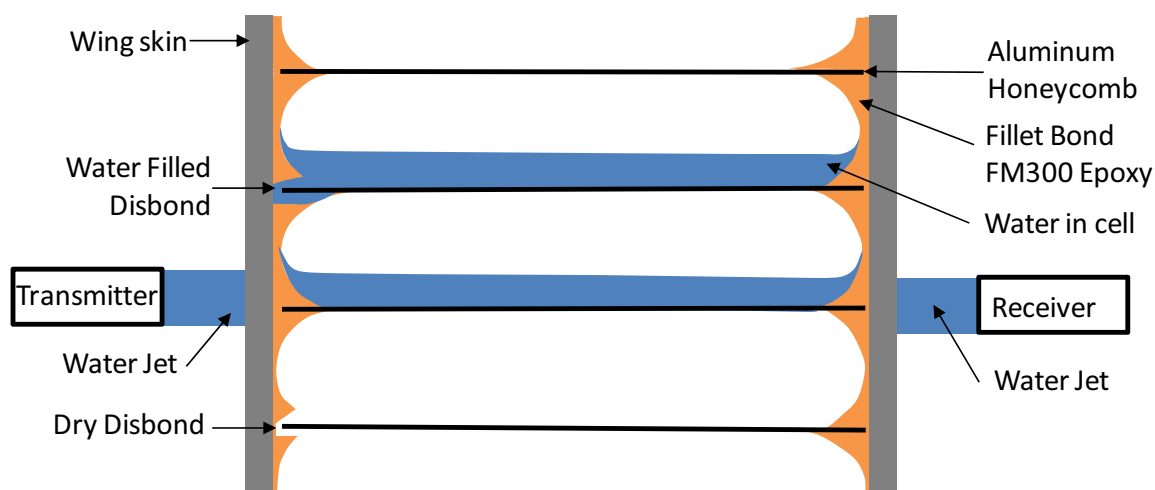


Fig. 1. Schematic side view of aluminum honeycomb cells with and without water

Acoustic energy is reflected or attenuated within the structure's components. Furthermore, the receiving transducer collects only that acoustic energy transmitted through the body of the sample that it is in line with to receive. Through-transmission UT is most often used to record time and loss of signal amplitude. For certain applications, this can be useful since a reduction in observed signal amplitude is sufficient to indicate an irregularity [9].

Evaluation of the ultrasonic signal is most easily conducted using an A-Scan display, where location of signals on the time-base is a function of distance and velocity of sound through the constituent materials [10]. The longitudinal sound velocities within the various components making up the rudder are shown in Table 1. Identification of the presence of water within the honeycomb structure is facilitated by the 4.3 times greater velocity of sound through the aluminum cell walls than though water, as shown in Table 1, resulting in a comparative later arrival of a second signal when water is present within cells.

As sound propagates through the composite material it is affected by the various material properties and interfaces between the composite constituents. At an interface, a fraction of the sound will pass through and the remainder will be reflected. The amount transmitted depends on the angle of incidence at the interface and the acoustic impedance (Z) of the two materials.

2. Theory

2.1. Ultrasound

The application of through-transmission ultrasonic testing for rudder inspection involves using separate aligned transducers (transmitter and receiver), with one on either side of the test material as shown in Fig. 1. Ultrasound is transmitted via a couplant to the carbon fiber/epoxy wing skin, through FM300 epoxy adhesive, aluminum honeycomb core and water, if it is present within the cells or within a disbond, and back out through the structure.

Table 1. Properties of materials (velocity of sound, density, and acoustic impedance)

Material	Velocity of Sound v (m/s)	Density ρ (kg/m ³)	Acoustic Impedance, $Z = \rho v$ (kg/m ² s) [11]
Aluminum	6320	2700	17×10^6
Water (20 °C) [12]	1483	998	1.48×10^6
Air (20 °C) [12]	343	1.204	413
Epoxy (Hysol C8-4143/3404)	2850	1580	4.52×10^6
Carbon Fibre/Epoxy Skin [13]	7600	1450	1.1×10^7

Acoustic impedance, Z , is the product of density, ρ , and velocity of sound, v , within the material, $Z = \rho v$ [11]. Densities and impedances of materials in the composite structure are shown in Table 1. For normal incidence the intensity, I_T , ultrasonic energy per unit area per unit time, transmitted across the boundary, expressed as a percentage in terms of source material, with impedance Z_1 , and receiving material, with impedance Z_2 , is [10]:

$$I_T = \left[\frac{4Z_1 Z_2}{(Z_1 + Z_2)^2} \right] (100\%). \quad (1)$$

As can be observed from Eq. 1, maximum ultrasonic energy transfer between two media occurs when their respective impedances are most closely matched [10]. Sound intensities transmitted across various interfaces within the composite rudder, estimated using Eq. 1, show that maximum transmission occurs between Carbon Fiber/Epoxy wing skin and Epoxy (83%), followed by water to Epoxy (75%), aluminum to Epoxy (66.4%) and aluminum to water (30%). Air, which simulates a dry disbond condition only transmits 0.01% of the sound intensity.

The total signal intensity transmitted through the structure may be estimated as the product of transmitted intensities at each interface given by:

$$I_{T_{\text{Total}}} = \prod_{i=1}^n I_{T_i} \quad 100\%. \quad (2)$$

Note that these estimates do not take into account internal reflections between layers within the composite structure. These may be expected to slightly increase the transmitted signal amplitude as well as contribute to spread of the signal in time. Transmission is also affected by the non-parallel surfaces of the rudder, which may introduce a 2° off-normal incident beam under ideal conditions. The aluminum honeycomb structure is made up of thin walls with thickness on the order of 0.03 mm (0.001"), limiting beam spread as the ultrasound is channeled along the thin laminar sheets of the honeycomb. Since the honeycomb varies in thickness over the rudder cross-section, attenuation is also a factor. The exponential decay of acoustic pressure with distance through the core may be expressed as [10]:

$$P = P_0 e^{(-\alpha L)}, \quad (3)$$

where P is the acoustic pressure at the second reference location, P_0 is the original acoustic pressure at the source, α is the attenuation coefficient in (dB per metre) and L is the distance travelled by the ultrasonic pulse from source to second reference location. The attenuation coefficient for bulk 6061-T6511 aluminum is 90 dB/m [10] and for water at 2.25 MHz can be calculated from [14] as 1.1 dB/m. Therefore, attenuation in the aluminum honeycomb core is expected to be greater. Note also that the thin walled core may cause additional attenuation due to its small cross-sectional area normal to the beam. The intensity defined in Eq. 1 may be related to maximum pressure amplitude P_{\max} and is given as [15]:

$$I = (P_{\max}^2)/2Z. \quad (4)$$

Therefore calculations of the intensity may be related to the peak amplitude squared and the impedance of the medium in which the ultrasound is traveling.

2.2. Thermography

Infrared thermography is used to measure and evaluate temperature variations in a material and represent them visually. In aerospace composite materials, with components that are properly bonded, laminated and free of inclusions, thermal characteristics such as diffusivity, conductivity and capacitance will be uniform across the surface. For regions where disbonding, delaminations or inclusions occur such as in the presence of water, varying thermal characteristics will be represented as a change in thermal signature on the image [16].

When a material is at a temperature that is different from its surroundings, a thermal gradient will arise that drives heat energy to equilibrium. The rate at which heat energy moves is a function of the thermal diffusivity of the material given by [16]:

$$K = (\rho C_p C_1 P), \quad (5)$$

where K is the thermal conductivity (W/m-K), ρ the density (kg/m³) and C_p the specific heat capacity (J/kg-K). Eq. 5 with values from reference [12] can be used to obtain the thermal diffusivity at 0°C of water ($1.333 \times 10^{-7} \text{ m}^2/\text{s}$) and ice ($1.38 \times 10^{-6} \text{ m}^2/\text{s}$), and that of aluminum ($1.029 \times 10^{-4} \text{ m}^2/\text{s}$), the relevant materials for examining thermographic variations in rudders with water ingress. Note that water has the lowest thermal diffusivity and highest heat capacity and therefore, is expected to have a greater effect on thermographic imaging. Therefore, the presence of water within cells of the honeycomb composite changes thermal properties in that area of the material. As a result, if a rudder is frozen and then allowed to return to room temperature, regions in which ice is present will warm more slowly than those without ice or water. The ice regions will then thaw, requiring a larger amount of heat (latent heat of fusion), and finally, warm to room temperature, but more slowly than areas with only aluminum. If a thermographic image is captured during this process, the result will be areas with a dark color that correspond to the lower temperatures that occur due to the presence of ice or water. Air forces that fly and maintain the F/A-8 incorporate this process by placing the rudder in a freezer until the water inside the cells freezes. The rudder is then placed at room temperature. The temperature of the structure will rise faster in regions without water, producing differences in temperature between regions with and without water.

2.3. Neutron radiography

Neutron radiography is an imaging technique which involves using neutrons to perform radiography on a test subject. Although neutron accelerators and radioisotopes provide a relatively portable source of neutrons, nuclear reactors provide a greater neutron flux, and therefore produce higher quality and more accurate images [5]. As neutrons travel through the material, they are attenuated according to the elements encountered in their path. The neutrons release their energy to a recording device placed behind the test object, producing a two dimensional image of the test object [5]. In contrast to X-radiography, where the attenuation of X-rays is a result of the target material's atomic number, neutrons are most strongly attenuated by elements with high mass attenuation coefficients such as Hydrogen (H), Boron (B), Gadolinium (Gd) and Indium (In) [17]. Neutron radiography is useful for the location of water in the honeycomb structure, since water is composed of a 2/3 atomic fraction of hydrogen. Aluminum and other materials in the structure have a weaker interaction and therefore, have a less dominant presence in the image [18].

3. Experimental technique

Through transmission ultrasonic C-Scan and thermography on a rudder removed from service due to water ingress were performed at the Quality Engineering and Test Establishment (QETE) in Hull, Quebec. Neutron

radiography examination and accompanying images were produced using the 20 kW Safe LOW Power critical Experiment (SLOWPOKE-2) reactor at the Royal Military College of Canada (RMC).

The ultrasonic system at QETE utilized a water-jet through-transmission (squirter[9]) set-up as schematically represented in Fig. 1. Ultrasonic energy was coupled from the transmit probe via the water jet through the component and via a second water jet to the receive transducer. The data acquisition and analysis system along with ultrasonic module was manufactured by TecScan (Boucherville, Quebec). The ultrasonic Panametrics transducers were 12.7 mm (0.5") in diameter with 2.25 MHz centre frequency. Transducers were precisely aligned using swivel gimbals in order to maximize through transmission energy. Total estimated path length for the ultrasound was fixed at 309 mm, unlike manual through-transmission inspection, where ultrasound coupled directly to the component material with coupling gel [7], experiences a varying path length as the thickness of the rudder changes.

Initial detection of water ingress was determined by application of thermography. The Infrared images of the rudder indicated the approximate locations of water ingress within the honeycomb core. The Infrared camera used was the FLIR ThermaCam P60, manufactured by FLIR Systems. The P60 camera uses 320 x 240 pixel Focal plane array (FPA) uncooled microbolometer detector and has a thermal sensitivity of up to 0.06°C at a temperature of 30°C. A full colour 640 x 480 pixel digital video camera is built in to allow for image capture. The P60 is capable of measuring temperature in a range from -40°C to +120°C with an accuracy of $\pm 2^\circ\text{C}$ or $\pm 2\%$ [19].

Neutron Radiography images were obtained by placing the rudder on a positioning table and capturing digital images using a Charge Coupling Device (CCD) camera. This produced a map of the exact locations of water ingress within the honeycomb cells of the rudder's core.

4. Results

Two rudders removed from service and identified here as Rudder #1 and Rudder #2, were examined for water ingress and potential disbond using thermography, neutron radiography and through-transmission ultrasonics.

In the field, thermographic images are used to provide initial evidence of the presence of water within the rudder. Figs 2a and 2b show thermographic images of the outboard portion of Rudder #1 after it was removed from a freezer and permitted to warm to room temperature. Fig. 2a shows an image with a temperature scale between -2 and 23°C. Fig. 2b, taken 2 minutes after Fig. 2a, is characterized by temperatures between 1 and 23°C. As Fig. 2a includes temperatures below 0°C, it likely captures regions of ice. In Fig. 2b temperatures are above 0 °C and therefore the indicated thermograph is attributed to water only. As water has the lowest thermal diffusivity (Eq. 5) and highest heat capacity [12] the distinction between regions with and without water are more clearly resolved in this image than when water is frozen as in Fig. 2a. The temperature gradient is not however, isolated to just the cells filled with water. The heat will diffuse through the structure and appear as broader areas of temperature difference, which

may be interpreted as larger regions of water ingress than actually exists. When comparing the visual results of Fig. 2a and 2b, there are clear similarities in the shape of the area of water ingress as observed in Neutron Radiography and Ultrasonic measurements, which follow. However, the resolution of the thermographic image is far less.

Neutron Radiography was carried out on the rudders and the resulting images were assembled as shown in Fig.3 below. The images demonstrate location and relative amount of water as darker regions within the honeycomb cells for a given exposure [20]. Less exposure (darker) is due to Neutron attenuation by hydrogen (water) contained within the cells of the rudder. Consistent with Fig. 2, the bulk of the water occurs near the upper hinge, as in the majority of the rudders that have been studied [21]. Additional water has also migrated towards the centre of the upper portion of the rudder, with a pattern that is similar to the thermography images shown in Fig. 2. Fig. 3 will be used again for comparison with ultrasonic results.

Through-transmission ultrasonic C-Scans of the rudder section were generated from A-Scans. C-Scans are based on representation of the maximum signal amplitude within a given time interval or gate by an amplitude dependent color scale and are plotted as a function of horizontal and vertical position [10]. Fig. 4 shows an ultrasonic C-scan of the rudder gated for water only. Observed patterns of water ingress are in agreement with those observed in the higher resolution neutron radiograph results. Fig. 5 shows an ultrasonic C-scan of the rudder gated for the aluminum path signal. The resultant peak amplitude pattern is modified in regions near the rudder hinges most generally associated with areas of disbond. This will be discussed further for Rudder #2 below.

Positions with and without water, were selected for display of A-scans from Rudder #1. The positions were located along a line approximately 40 mm from the leading edge in order to maintain similar core thickness. Figs 6a through 6d show A-scans with gates set between 45 and 56 μs , the nominal position for time of signals that have passed through water within cells. Fig. 6a shows an A-Scan from a location where water was absent. In Fig. 6b the aluminum honeycomb signal amplitude is weak, indicating poor coupling of sound that may be attributed to degraded bonding. Fig. 6c shows two signals, the first associated with aluminum and the second occurring later in time and therefore associated with water in the cell. Fig. 6d shows two signal amplitudes, but with the aluminum signal considerably weaker than that observed in Fig. 6c at about the same thickness of rudder.

A second rudder, Rudder #2, with more localized water ingress, was also examined. Fig. 7 shows the infrared thermography, neutron radiography and through-transmission ultrasonic C-Scans gated separately for water and aluminum prior to drying out the rudder (pre-dry) and after the rudder had been dried out (post-dry), following a vacuum bag procedure described in [5]. Thermography, neutron radiography and ultrasound show water ingress between the two hinges along the titanium spar. Thermography again shows a much more dispersive representation of water ingress than either of the other two techniques. The highest resolution, allowing identification of water in separate cells, is provided by neutron

radiography. Unfortunately, the quality of the ultrasound signal, gated for aluminum, did not permit the clear identification of reduced coupling observed in Rudder #1. However, a post-dry C-Scan, permitted clear identification

of regions of disbond, identified as a suppression of the through-transmitted signal. The extent of this region closely matched that of regions where water was observed within Rudder #2 as observed in Fig. 7c.

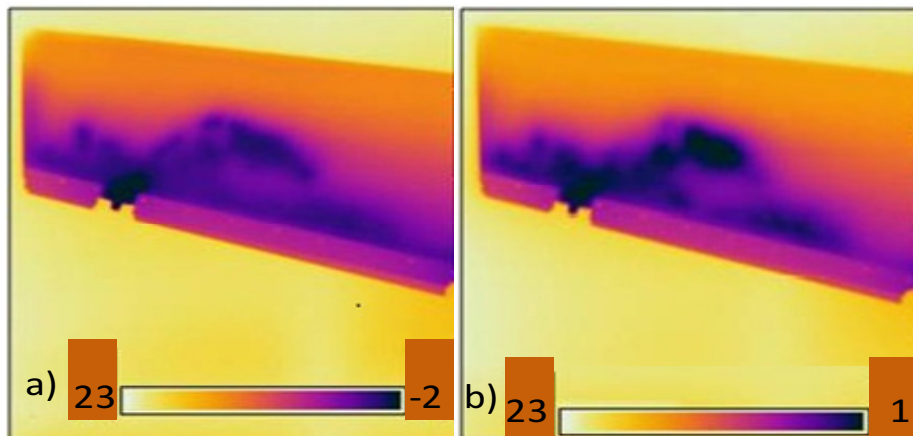


Fig. 2. Thermography image of rudder a) initial and b) 2 minutes later (temperature scale in °C).



Fig. 3. Compiled images of neutron radiography of rudder #1 (rudder top is to the left)

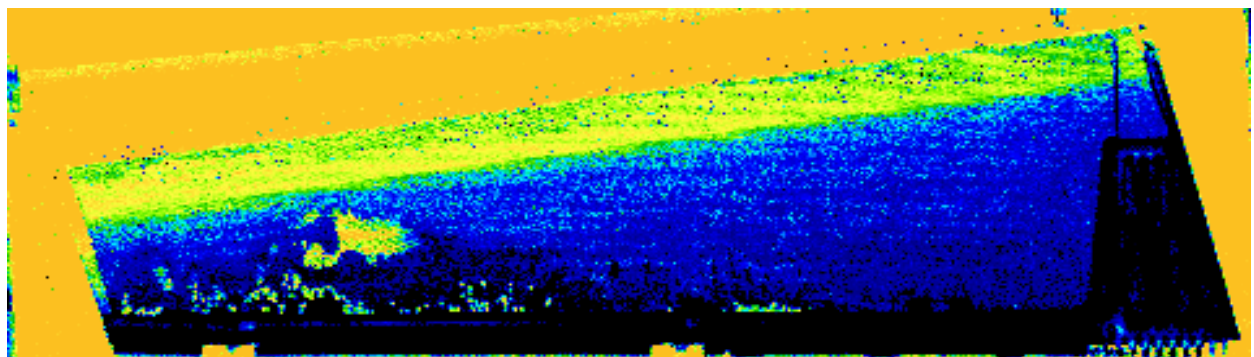


Fig. 4. Through transmission C-scan of rudder #1 Gated to show water signal (rudder top is to left)

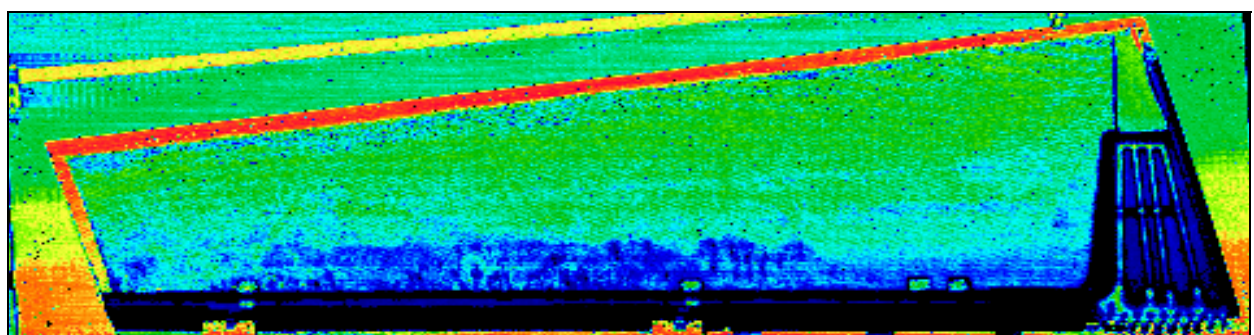


Fig. 5. Through transmission C-scan of rudder #1 Gated to show aluminum signal (rudder top is to left)

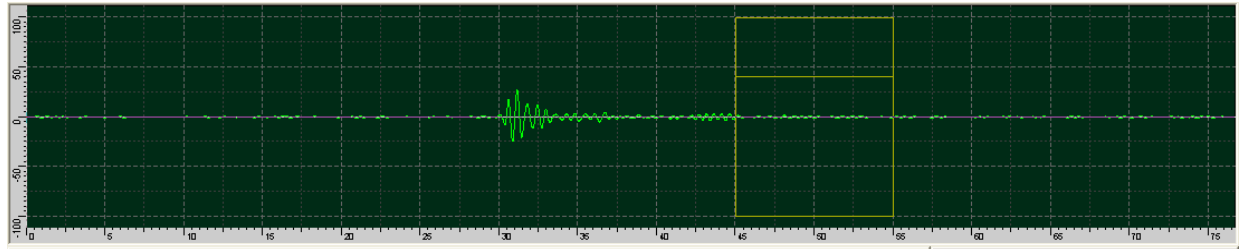


Fig. 6a. A-scan with no water taken at 40 mm from leading edge and 90 mm from top

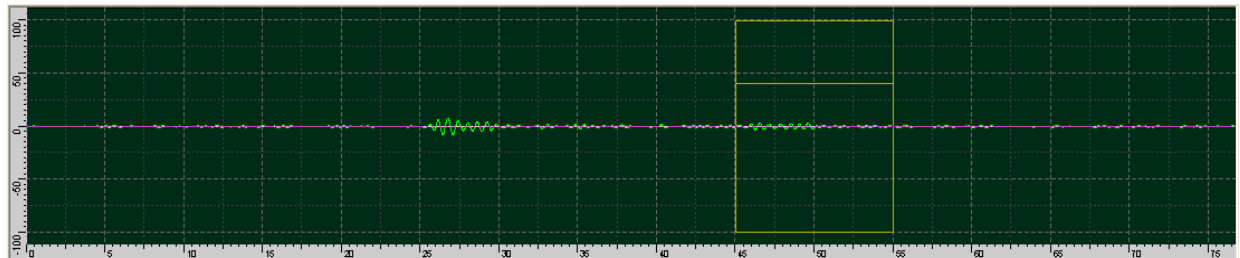


Fig. 6b. A-scan showing disbond at 40 mm from leading edge and 40 mm from top

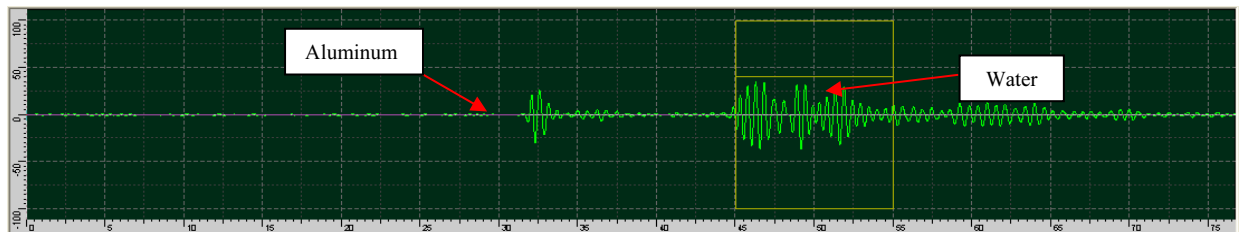


Fig. 6c. A-scan showing aluminum and water signals at 40 mm from leading edge and 350 mm from top of rudder

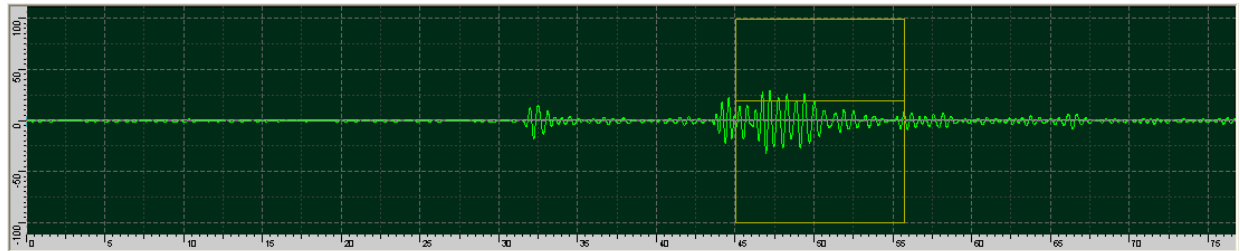


Fig. 6d. A-scan showing reduced aluminum and water signal taken at 40 mm from leading edge and 530 mm from top of rudder

5. Analysis and Interpretation

The water-jet system provides a fixed path length for through-transmission ultrasound in the rudder, in contrast to the application of surface transducers where the variable rudder thickness results in a more significant variation of signal arrival times. The fixed path length permits the clear differentiation between aluminum and water path signals in A-Scans when water is present, since the changing rudder thickness can be more easily compensated for.

The reduction in amplitude of the ultrasound signal within the composite structure can be examined in light of the various interfaces between composite components within the rudder, the presence of water with and without disbond and the attenuation of the signal through the

varying thickness of the honeycomb. Fig. 1 is used to depict possible scenarios for reduction in through-transmission amplitude. These may be combined with representative A-scans in Fig. 6a through 6d resulting in the following proposed paths for ultrasound:

1. Intact bond at epoxy-to-aluminum interface and no water in cell (Fig. 6a).
2. Complete disbond with no water present in cell (Fig. 6b).
3. Intact bond with epoxy-to-aluminum interface at the water-filled cell (Fig. 6c).
4. Disbond between honeycomb and carbon/epoxy skin with water in the cell, implying an epoxy-to-water and water-to-aluminum path for sound (Fig. 6d).

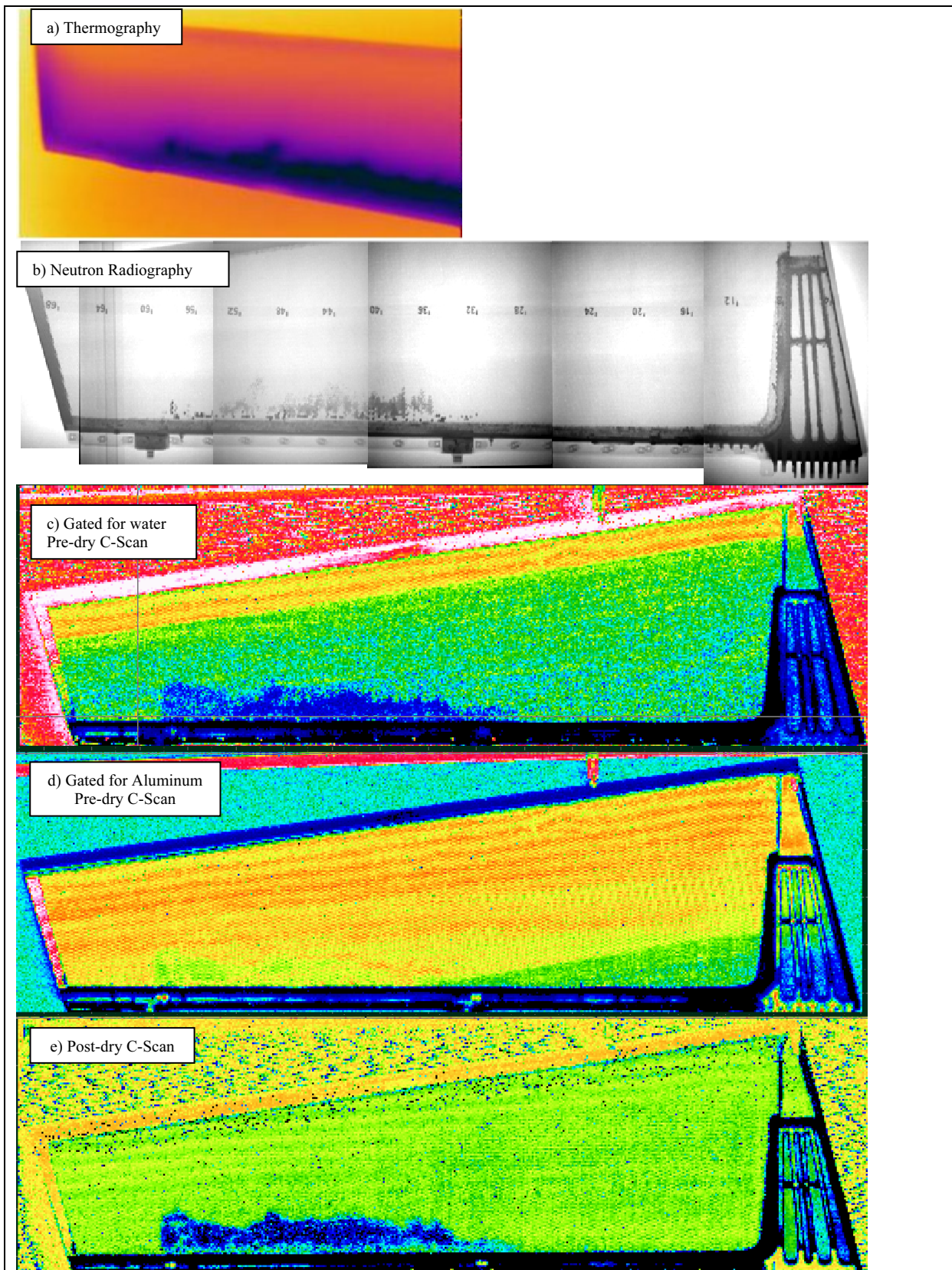


Fig. 7. Comparison of a - infrared thermography, b - neutron radiography and through-transmission ultrasound C-scans c - gated for water, d - gated for aluminum, and e - post-dry C-scan for rudder #2 (top of rudder is to the left)

While the presence of a dry disbond will severely limit the amount of sound transmitted, as demonstrated by a comparison of Figs 6a and 6b, the introduction of water in the disbonds will facilitate transmission of sound through the composite structure. However, the change and addition of an interface for water within a disbonds (case 4 above) will result in reduced signal amplitudes. This is demonstrated by a comparison of relative transmitted sound intensity between cases 3 and 4 using Eq. 2. Under conditions of disbonds in the presence of water, the epoxy-to-aluminum interface in Case 3 (intact bond) is replaced by epoxy-to-water and water-to-aluminum interfaces as described for Case 4. The ratio of through transmission intensity in Case 3, I_{3T} , to the Case 4 intensity, I_{4T} , becomes a ratio of epoxy-to-aluminum interface intensity, $I_{\text{epoxy/aluminum}}$, to the product of intensities of epoxy-to-water and water-to-aluminum, $I_{\text{epoxy/water}} \times I_{\text{water/aluminum}}$. Since the other interfaces remain unchanged, the ratio of through-transmission intensities becomes:

$$\frac{I_{3T}}{I_{4T}} = \frac{\prod_{i=1}^n I_{aT_i}}{\prod_{i=1}^m I_{4T_i}} = \frac{I_{\text{epoxy}}}{I_{\text{aluminum}}} \times \frac{I_{\text{water}}}{I_{\text{aluminum}}} = \frac{0,66}{0,75 \times 0,30} = 3 \quad (6)$$

where I_{3T_i} and I_{4T_i} are the transmitted intensities at the i^{th} interface for each case. These calculations indicate that although the presence of water acts as a couplant for sound through the rudder, it only couples approximately one third of the sound intensity that a fully intact epoxy bond would. Eq. 7 may be written in terms of a ratio of maximum pressures using Eq. 4 and noting that receive transducer impedance, z , is constant for received signal responses. Therefore, in the case that disbonds with water is present the relative maximum amplitudes are reduced by the factor $P_{\max_1} / P_{\max_2} = \sqrt{3} = 1.7$. This reduction may be seen in an examination of relative aluminum signal amplitudes shown in Figs 6c and 6d (1.2/0.7=1.7), corresponding to cases 3 and 4 above, and is reflected in the C-Scan, Fig. 5, which shows regions of reduced aluminum signal amplitude near the hinge area. Note that the central rudder region, where substantial water was detected, is not present in Fig. 5, suggesting that disbonds have not occurred although water is present. The central region therefore, may be a result of diffusion ingress of water a mechanism suggested by Radtke et al. [2]. While reduced coupling for through-transmitted signals, resulting in lower signal amplitudes, may be indicative of fillet bond degradation, further study is required to relate signal amplitudes to remaining bond strength.

6. Conclusions

As the presence of water is a degradation mechanism within composite structures, its detection may be used to identify potentially compromised structures. In this study of two F/A-18 rudders water within honeycomb cells was observed with highest resolution using neutron radiography, followed by through-transmission ultrasonics and finally thermography, where water indications were much more diffusive. Association of earlier-in-time

ultrasonic signals within A-scans with the aluminum honeycomb component of the structure permitted their differentiation from the later-in-time water signals. The first rudder in the study was characterized by significant water ingress, observed in its hinge region and its central top section. The second rudder demonstrated water primarily at the leading edge between its two uppermost hinge locations. Water removal, by drying of the second rudder, confirmed presence of disbonds in the hinge region, where significant direct water ingress had occurred.

A model of the effect on peak ultrasonic signal amplitude, under conditions of disbonds between FM73 epoxy adhesive and aluminum, in the presence of water, was developed. The model predicted a 60% reduction in observed peak signal amplitude when disbonds in the presence of water occurred. Qualitative evaluation based on examination of C-Scans gated for aluminum path signals provided evidence of reduced peak amplitudes of this order in the hinge region of both rudders. In the central portion of the first rudder, where water was also observed and presumed to be present by diffusion rather than direct ingress, reduced amplitudes were not present, suggesting that bonds in this region could be intact. These results suggest that the presence of disbonds may be identified by observation of a relative reduction in ultrasonic signal amplitude.

Acknowledgements

The first two authors would like to thank Chun (Lucy) Li and A. Tetervak for useful discussions. This work was supported by the Department of National Defence and the Natural Science and Engineering Research Council of Canada.

References

1. Shirrell C. D., Leisler W. H. and Sandow F. A. Moisture induced surface damage in T300/5208 graphite/epoxy laminates. Nondestructive Evaluation and Flaw Criticality for Composite Materials. ASTM STP 696. R. B. Pipes, Ed., American Society for Testing and Materials. 1979. P. 209.
2. Radtke T. C., Charon A. and Vodicka R. Hot/wet environmental degradation of honeycomb sandwich structure representative of F/A-18: Flatwise Tension Strength. DSTO Aeronautical and Maritime Research Laboratory. 1999.
3. Flight safety incident. Report 94844, CF188725, 441 Sqn, 4 Wing Cold Lake. 23 March 1999.
4. E-mail from Richard Gagnon. Life Cycle Material manage Flight Control Surfaces and landing Gear Doors to Capt Hungler. 25 April 2007.
5. Hungler P. L. Development and evaluation of a water removal technique for the CF188 Rudder. M.A.Sc Thesis. Department of Chemistry and Chemical Engineering. Royal Military College of Canada, Ontario, Canada. May 2008. P. 35.
6. Li C., Teuwen J. and Lefebvre V. Investigation of moisture ingress and migration mechanisms of an aircraft rudder composites sandwich structure. Society for the Advancement of Material and Process Engineering. 2006.
7. F18-BSD-AYB-1045. F/A-18 Fleet Support Team NAVAIR North Island, CA. 8 Dec 2004.
8. Baldev R., Jayakumar T. and Thavasimuthu M. Practical Non-Destructive Testing. Narosa Publishing House. 2002. P. 77.
9. Mal A. K. University of California, Los Angeles and the ASM Committee on Ultrasonic Inspection. Ultrasonic Inspection. Metals Handbook Ninth Edition. Nondestructive Evaluation and Quality Control. Revised by Bar-Cohen, Y., Douglas Aircraft Company, McDonnell Douglas Corporation. Vol. 17. P. 289.

10. **Bray D. E. and Stanley R. K.** Nondestructive Evaluation: a Tool for Design, Manufacturing and Service. McGraw Hill. 1989. Ps. 64, 71, 72, 94.
 11. **Matthews F. L., Rawlings R. D.** Composite materials: Engineering and Science. Woodhead Publishing. 1999. P. 416.
 12. **Lide D. R.** CRC Handbook of Chemistry and Physics 75th Ed. © 1995. Boca Raton. P. 16-1, 6-18.
 13. **Kim H. C., Park J. M.** Ultrasonic wave propagation in carbon-fibre reinforced plastics. Physics Department, The Korea Advanced Institute of Science and Technology, Chongyangri, Seoul, Korea. 15 May 1987.
 14. **Kinsler L., Frey A., Coppens A. and Sanders J.** Fundamentals of Acoustics. Third Edition, NewYork, John Wiley and Sons. 1982. P.148.
 15. **Serway R. A. and Jewett Jr. J. W.** Physics for Scientists and Engineers with Modern Physics, 6th Ed. (© 2004. Thomson Brooks/Cole, Belmont CA). P. 518.
 16. Annual Book of ASTM standards 2004, ASTM E 748-95, Standard Practices for Thermal Neutron Radiography of Materials. Metals Test Methods and Analytical Procedures. Nondestructive Testing, ASTM Subcommittee E07.05. Vol 03.03. P. 361.
 17. French Atomic Energy Commission. Neutron Radiography: Non destructive Testing. retrieved on 10 January 2010 from <http://www-lrb.cea.fr/neutrono/nrl.html>.
 18. **Harms A. A and Wyman D. R.** Mathematics and physics of neutron radiography. D. Reidel Publishing, Holland. 1986. P. 2.
 19. FLIR Thermography. FLIR Infrared Cameras. retrieved 15 January 2010 from www.flirthermography.com/P60data.
 20. **Tang B. P. Y.** A reliability study of neutron radiology as applied to CF188 rudder water ingress. M. A. Sc Thesis. Department of Chemistry and Chemical Engineering, Royal Military College of Canada, Ontario, Canada. May 2006. P. 8.
 21. **Li C., Ueno R. and Lefebvre V.** Investigation of an accelerated moisture removal approach of a composite aircraft control surface. Society for the Advancement of Material and Process Engineering. 2006.
- A. K. Edwards, S. Savage, P. L. Hungler, T. W. Krause
- Lėktuvų F/A-18 korinių kompozitinių krypties vairų atsisluoksniaivimo dėl vandens tyrimas ultragarsiniu pereigos metodu**
- Reziumė
- F/A-18 lėktuvo krypties vairo plokštumos gaminamos iš anglies pluošto paviršinių sluoksnių ir aluminio korinės struktūros kompozitų, kurie yra jautrūs vandens įsiskverbimui. Skrydžio metu nulūžo vairo plokštuma dėl įsiskverbusios drėgmės sukelto atsklajavimo defekto tarp paviršinio kompozito sluoksnio ir korinės struktūros. Rankinis ultragarsinio tyrimo metodas, pritaikytas vairo plokštumos tyrimui, aptinka atsklajavimą pagal priimto signalo amplitudės sumažėjimą. I korinės struktūros ertmes įsiskverbės vanduo pagerina ultragarso pereigą, bet apsunkina atsklajavimo vietos aptikimą. Šiame darbe vanduo buvo aptiktas eksplloatuojamuose vairuose naudojant termografiją. Tikslios vandens įsiskverbimo vietos buvo aptiktos taikant neutronų radiografijos metodą. Atlikus laiko srities analizę, tiesioginės pereigos metodu ir taikant vandens srautą išmatuotuose A signaluose, nustatyti skirtumai tarp vandeniu užpildytų korinės struktūros kiaurymių (defektų) ir korinės struktūros sienelių skiriamosios ribos. Įvertinus nuo korinės struktūros sienelių atspindėtų signalų amplitudes, sumodeliavus nesusiklajavimą ir vandens įsiskverbimą, nustatytos potencialios galimybės aptiki korinės struktūros defektus esant vandens įsiskverbimui.

Submitted 29 04 2011